J. Fluid Mech. (1983), *vol.* 137, *pp.* 153–164
Printed in Great Britain

Boundary-layer transition and the behaviour of spiral vortices on rotating spheres

By Y. KOHAMA AND R. KOBAYASHI
Institute of High Speed Mechanics, Tohoku University, Sendai, Japan

(Received 29 June 1983)

The mechanism of boundary-layer transition and the behaviour of spiral vortices on spheres rotating in otherwise undisturbed fluid were investigated experimentally. Critical and transition Reynolds numbers which determine the laminar–turbulent transition regime on the sphere surface were measured. In addition the number of spiral vortices on the sphere and the direction of the vortex axis were clarified.

1. Introduction

When a sphere is rotating with constant angular velocity about a diameter in otherwise undisturbed fluid, a flow is induced around the surface of the sphere from the two poles toward the equator, by fluid viscosity, and then radially away from the equator. The resulting stationary flow is three-dimensional. The induced flow is of fundamental interest in the fields of meteorology, astrophysics, fluid dynamics, and many others. Howarth (1951) first investigated this problem theoretically (limited to the case of laminar flow), introducing a boundary-layer approximation. Since then, many scientists (Nigam 1954; Stewartson 1955; Kobashi 1957; Bowden & Lord 1963; Kreith *et al.* 1963; Banks 1965, 1976; Manohar 1967; Singh 1970; Sawatzki 1970; Yamabe, Nishida & Ito 1982) have worked on this problem, both theoretically and experimentally, and the structure of the flow field in the case of a laminar boundary layer has been greatly clarified.

However, the actual flow field around a rotating sphere involves in general not only a laminar boundary layer, but also a transition regime and a turbulent boundary layer. Sawatzki (1970) first investigated this whole flow field experimentally, and detected sinusoidal velocity fluctuations using hot-wire anemometry in the laminar boundary layer before transition to turbulence. He presumed that the same kind of spiral vortices that occur on a rotating disk might be appearing in this region. Also he found that the transition regime shifts toward the pole with rotating speed, and measured several properties of the vortices.

The purpose of this report is to determine the position of the transition regime as a function of the spin Reynolds number and to clarify the structure of spiral vortices and their breakdown process to the turbulent state in detail.

2. Experimental apparatus and procedure

Three aluminium spheres of different sizes were tested. Their diameters were $D = 250$ mm, 150 mm, 70 mm, and their surfaces were finished smooth and painted black. The test sphere was horizontally mounted on a shaft placed 800 mm above the floor level in a large closed room and was driven by a d.c. motor through a V-belt in otherwise undisturbed air. The rotation speed could be controlled continuously up to 3820 rev./min.

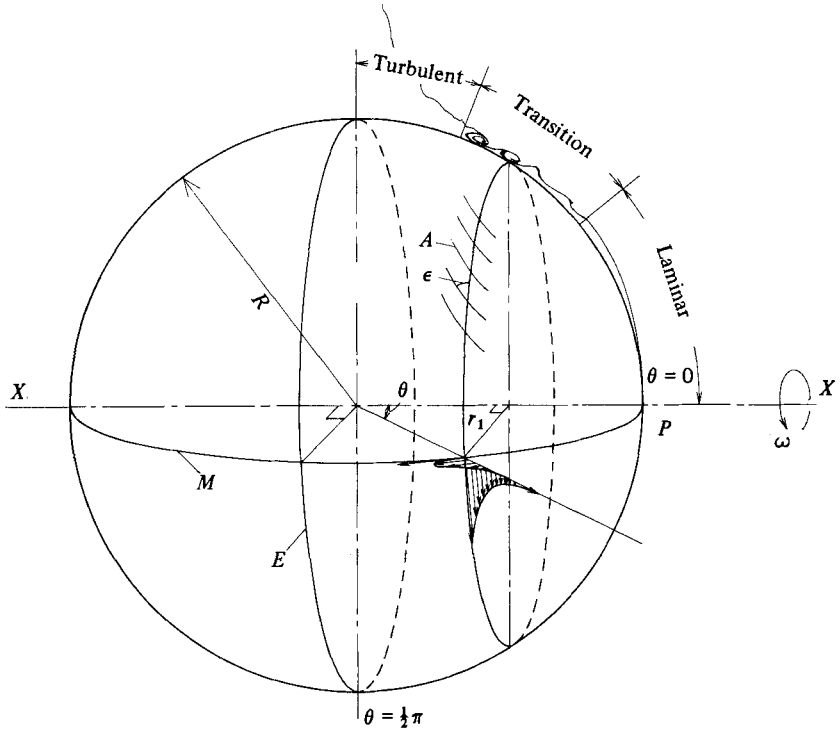

FIGURE 1. Rotating sphere and notation: E, equator; P, pole; M, meridian; A, vortex axis, X–X, axis of rotation.

The velocity field around the test sphere was measured by hot-wire anemometry, and flow patterns of the boundary layer on spheres were visualized by spreading titanium tetrachloride on the sphere surfaces. Vertically cut pictures of the transition regime in the boundary layer containing spiral vortices were taken by a slit-light stroboscope and a close-up camera. All photographs shown in the present paper are negatives in order to show the phenomena clearly.

Figure 1 illustrates the flow field of the rotating sphere and the notation. The spin Reynolds number is defined as $Re = \omega R^2/\nu$, where ω is the angular velocity, ν is the kinematic viscosity and R is the radius of the test sphere.

3. Experimental results and discussion

3.1. *Observation of the transition regime*

Figure 2 shows a typical flow pattern of the 250 mm-diameter test sphere rotating in a counterclockwise direction at a speed $N = 3200$ rev./min. In this photograph, one can see regularly arranged spiral vortices in the transition regime between the laminar boundary layer near the pole and the turbulent boundary layer near the equator. This transition regime shifts from the equator toward the pole with increasing rotation speed N.

Figure 3 shows a cross-sectional picture of spiral vortices appearing in the transition regime, which was taken by the slit strobolight set along the longitude. All the spiral streaks in figure 2 were thereby found to consist of vortices curling in the same direction.

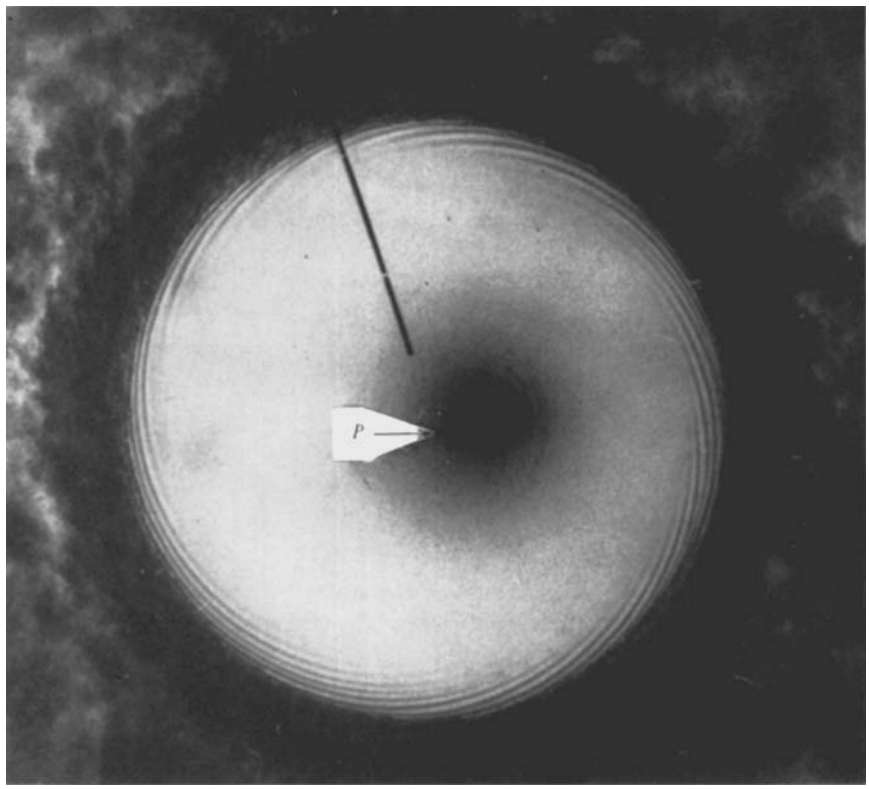

FIGURE 2. Visualized boundary-layer flow around a rotating sphere: $D = 250$ mm, $N = 3200$ rev./min, $Re = 1.83 \times 10^5$, P is the pole. (The radial line painted on a sphere is for reference.)

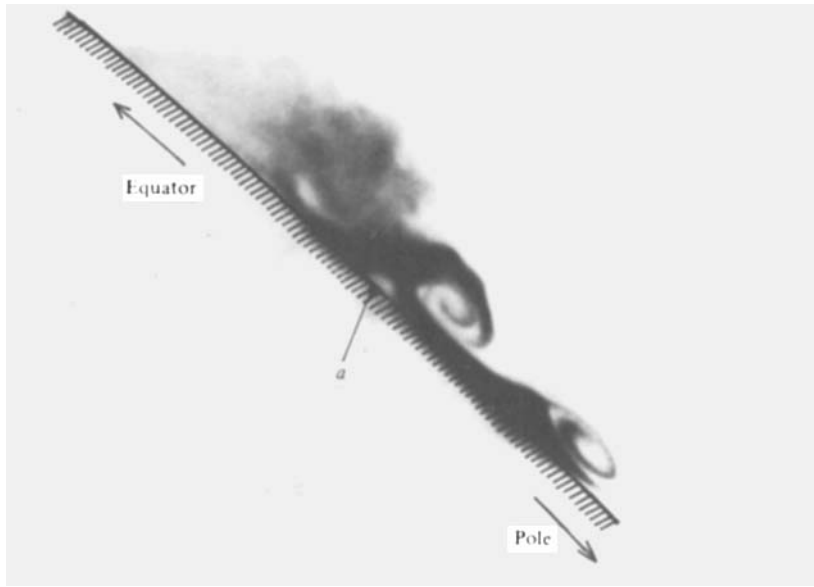

FIGURE 3. Cross-sectional picture of spiral vortices; $D = 250$ mm, $N = 1500$ rev./min, a is the surface of the sphere.

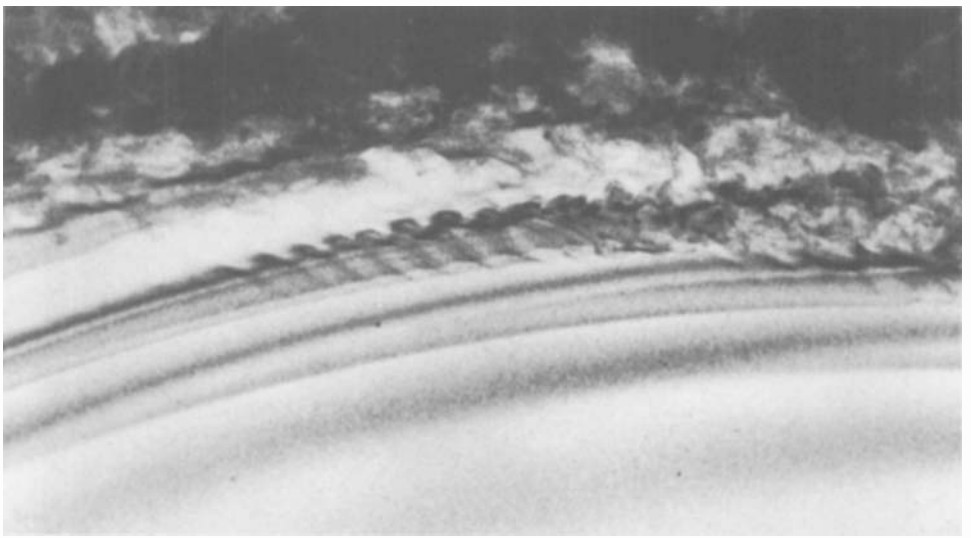

FIGURE 4. Approach shot of a spiral vortex; $D = 250$ mm, $N = 1500$ rev./min.

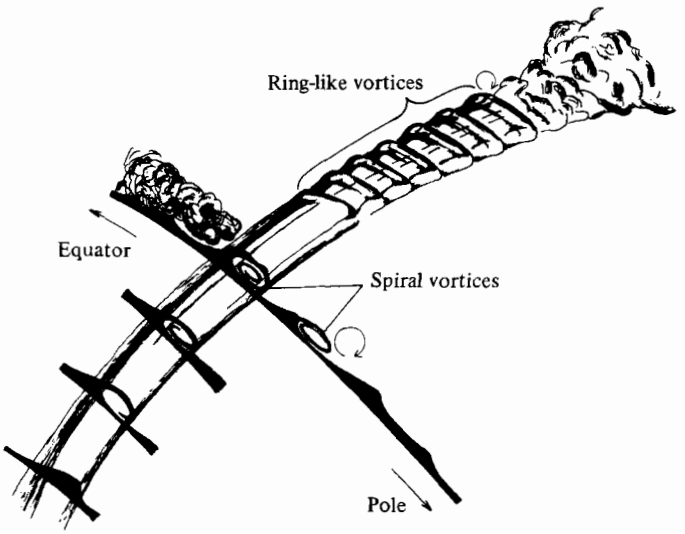

FIGURE 5. Sketch of spiral vortices.

The vortices look like those appearing on a rotating disk (Kobayashi, Kohama & Takamadate 1980) and on a rotating 30° cone (Kobayashi, Kohama & Kurosawa 1983), and differ from Taylor–Görtler vortices (Ito 1980), which curl in alternately opposite directions. It was found from some measurements of velocity profiles through the boundary layer that the sizes of the spiral vortices are nearly the same as the thickness of the boundary layer there.

Figure 4 is an approach shot of a process from the spiral vortex to the turbulent state. One can observe that a wavy instability occurs along the surface of the spiral vortex in the axial direction, and the disturbances then develop into ring-like vortices. All these superposed ring-like vortices are seen to curl in the downstream

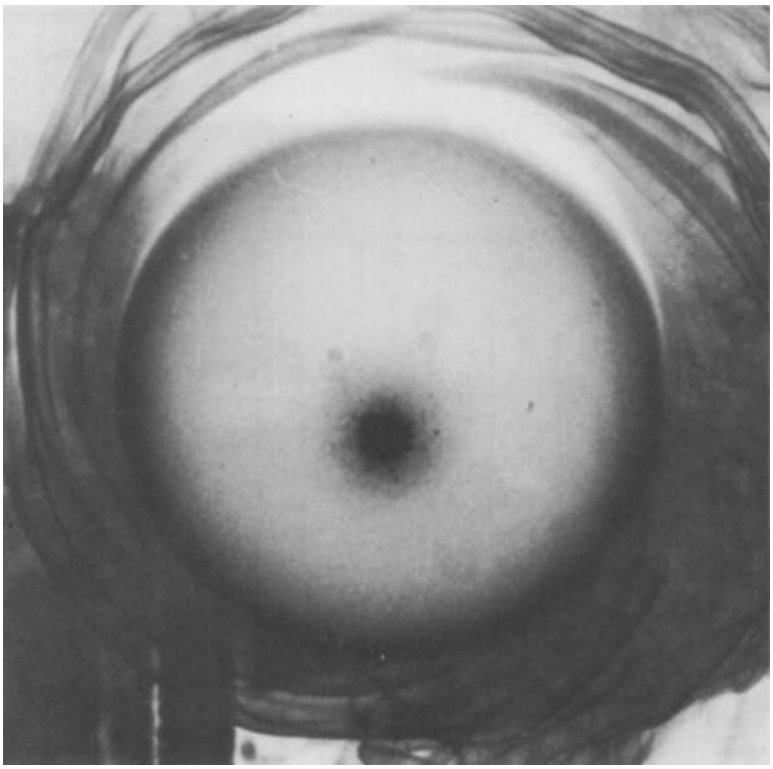

FIGURE 6. Flow around a sphere when the spin Raynolds number is small; $D = 70$ mm, $N = 500$ rev./min, $Re = 6.08 \times 10^4$.

direction. Figure 5 shows a sketch of the transition process, which was drawn with reference to many similar experimental evidences.

As shown in figure 6, one can also see spiral vortices flowing out radially from the equator, even if the whole surface of the sphere is covered with a laminar boundary layer in the case of small spin Reynolds number. One of the possible reasons for this is as follows. The portion near the equator is subject to centrifugal instability of the Taylor–Görtler-vortex type. Actually, in the case of a circular cylinder rotating with constant angular velocity in a still fluid, the critical Reynolds number for instability of Taylor–Görtler-vortex type is small (of order 10 in magnitude: Theodorsen & Regier 1944; Walowit, Tsao & DiPrima 1964; Kirchner & Chen 1970). If one regards a narrow band of the boundary layer along the equator of a sphere as part of a rotating cylinder, it can be said that the boundary layer near the equator of a sphere is quite unstable.

3.2. *Critical and transition Reynolds numbers*

We studied the parameters of the transition regime quantitatively in detail. Figure 7 (*a*) shows a distribution of turbulent intensity and variations of velocity fluctuating signals from laminar boundary layer to turbulent boundary layer along a longitude on the $D = 250$ mm sphere rotating at $N = 1200$ rev./min. Here the point of instability θ_c was measured as a state where the periodic signals resulting from the spiral vortices are just detected on frequency spectra, while the point of transition θ_t was defined as the state where the velocity fluctuations just lost the periodicity

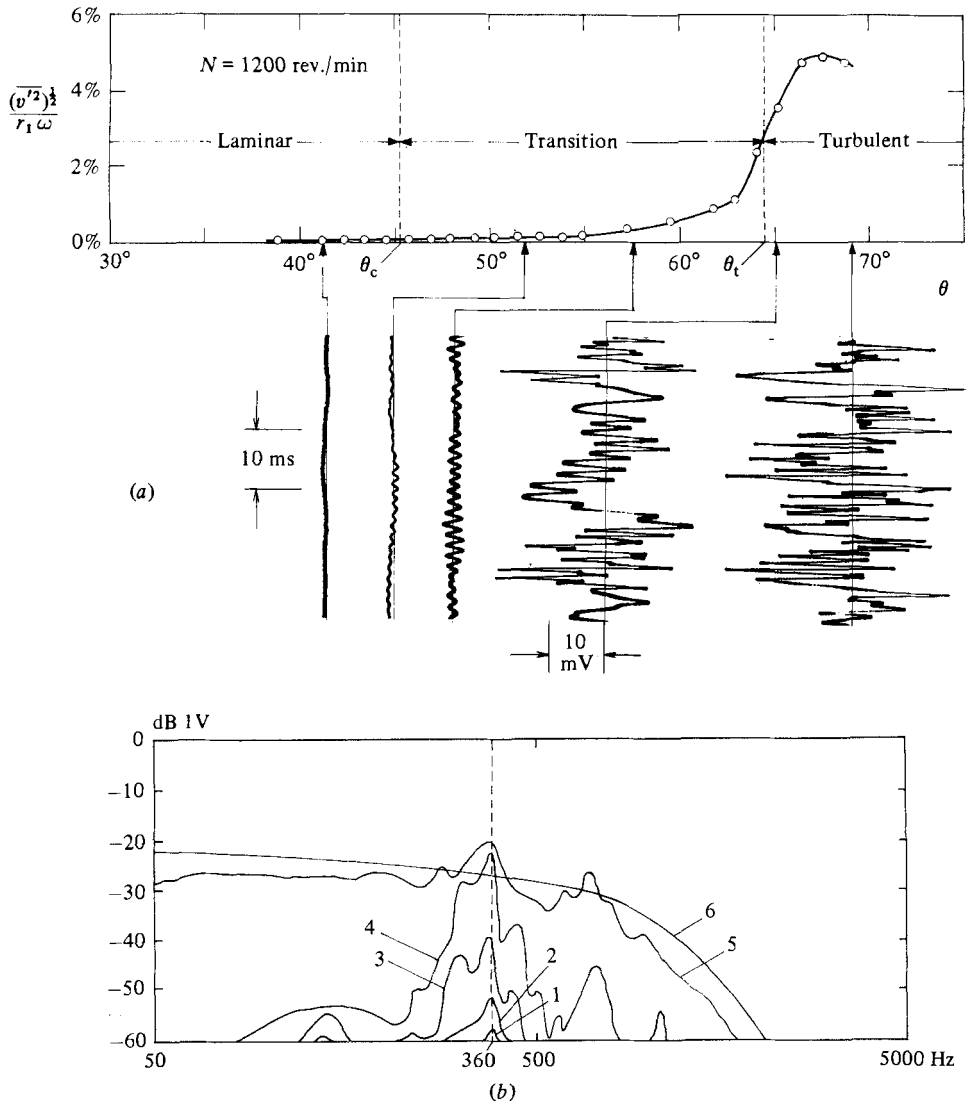

FIGURE 7. (*a*) Variation of velocity fluctuations in the transition regime along the longitude; $D = 250$ mm, $N = 1200$ rev./min. (*b*) Frequency spectra of the velocity fluctuations through the transition range; $D = 250$ mm, $N = 1200$ rev./min, $\theta_c = 45.3°$, $\theta_t = 64.2°$: (1) $\theta = 47°$; (2) 55°; (3) 57.5°; (4) 60°; (5) 63°; (6) 69.5°.

entirely. In figure 7 (*a*) sinusoidal velocity perturbations corresponding to the spiral vortices can be seen in the transition regime, and the magnitude of the turbulence intensity rapidly becomes large at the last stage of the transition. Here $(\overline{v'^2})^{\frac{1}{2}}$ is the root of the mean square of the velocity fluctuations in the latitudinal direction. In figure 7 (*b*) flow spectra at five stages through the transition range are shown together with the turbulent boundary-layer.

Figure 8 shows the location θ of the transition regime versus N, which begins at the point of instability θ_c and ends at the point of transition θ_t. It is clear from figure 8 that the transition regime shifts from the equator ($\theta = 90°$) toward the pole ($\theta = 0°$) with increasing rotation speed N, and that the location of the transition regime differs considerably among the three spheres at the same rotation speed N.

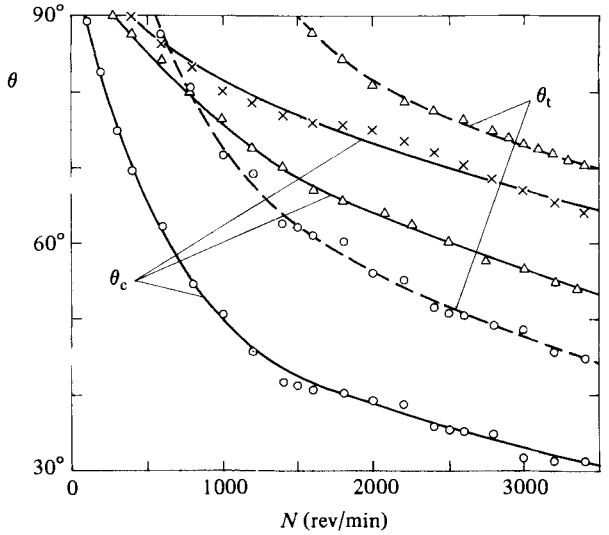

FIGURE 8. Variation of the critical point θ_c and the transition point θ_t with rotation speed N: ○, $D = 250$ mm; △, 150 mm; ×, 70 mm.

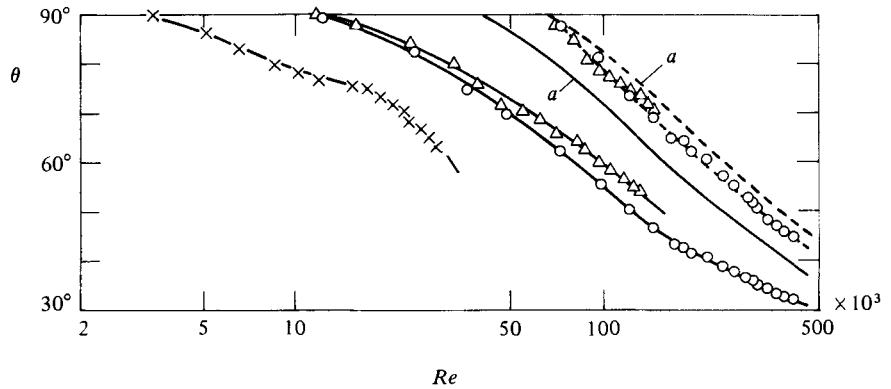

FIGURE 9. Variation of the critical point θ_c and the transition point θ_t with spin Reynolds number: —, θ_c; ------, θ_t; ○, $D = 250$ mm; △, 150 mm; ×, 70 mm; *a*, 240 mm (Sawatzki 1970).

Figure 9 gives the critical point θ_c and the transition point θ_t in relation to the spin Reynolds number Re $(= \omega R^2/\nu)$; the results of Sawatzki (1970) are also shown for comparison. Transition points for the three different spheres are almost identical, but the critical points vary considerably. Critical values θ_c measured by Sawatzki for the $D = 240$ mm sphere are large compared with ours. One of the possible reasons for this is the different sensitivity for detection of the critical condition.

Figure 10 shows the local Reynolds numbers $Re_{xc} = (\omega\theta_c R^2/\nu)\sin\theta_c$ and $Re_{xt} = (\omega\theta_t R^2/\nu)\sin\theta_t$ versus the rotation speed N, where $R\theta_c$, $R\theta_t$ are the distances measured along the sphere surface from the pole to the critical or transition points, and $\omega R\sin\theta_c$, $\omega R\sin\theta_t$ are the local peripheral velocities there. It is already known in the cases of a rotating disk (Kobayashi *et al.* 1980) and rotating cone (Kobayashi & Izumi 1979) that the local Reynolds numbers Re_{xc}, Re_{xt} remain unchanged as the rotation speed N is increased. It should therefore be noticed from figure 10 that, in the case of a rotating sphere, these local Reynolds numbers for the transition regime are seen to depend largely not only on the rotation speed N but also on the diameter

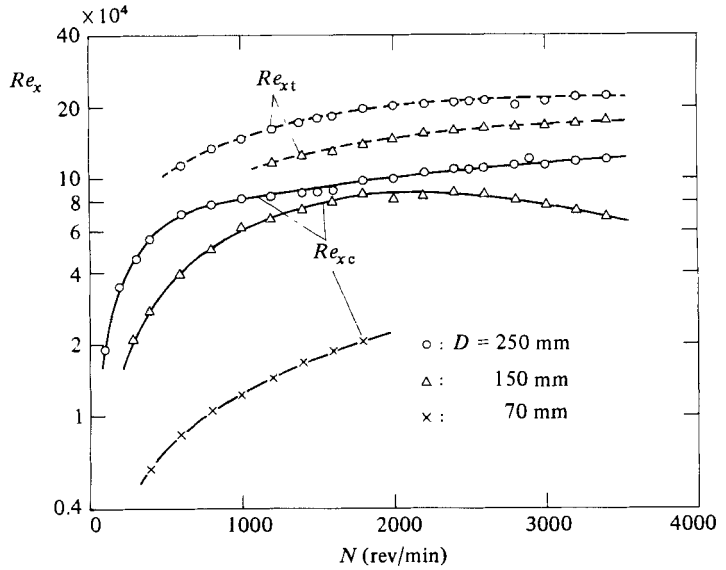

FIGURE 10. Local Reynolds number Re_x for transition regime versus rotation speed N: —, Re_{xc}; -----, Re_{xt}.

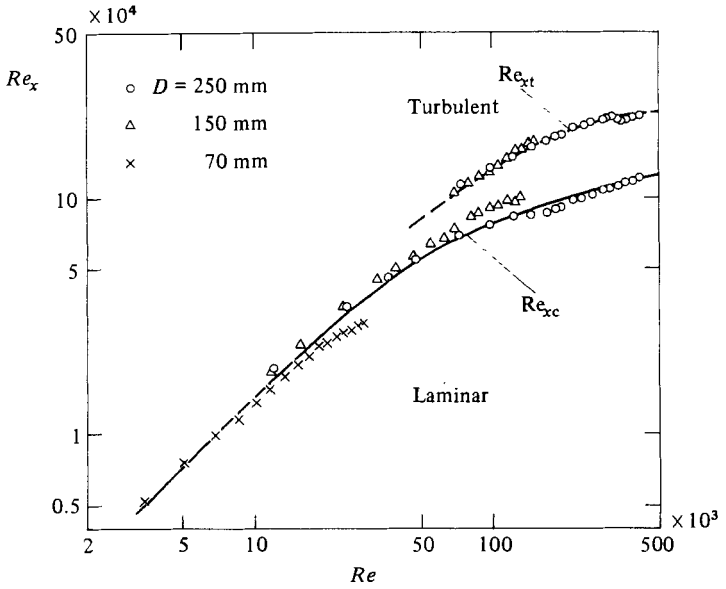

FIGURE 11. Local Reynolds number Re_x for transition regime versus spin Reynolds number.

of the sphere. A qualitative explanation for this is as follows. When N is small, the transition regime appears near to the equator, where the force balance in the boundary layer becomes similar to that of the rotating cone with small total angle, the boundary layer of which is more unstable than that with large total angle: the boundary layer thus becomes more unstable. As N becomes large, the transition regime shifts towards the pole, where the force balance becomes similar to that of the rotating disk: the values of Re_{xc} and Re_{xt} thus become large and approach asymptotically the values of the rotating disk.

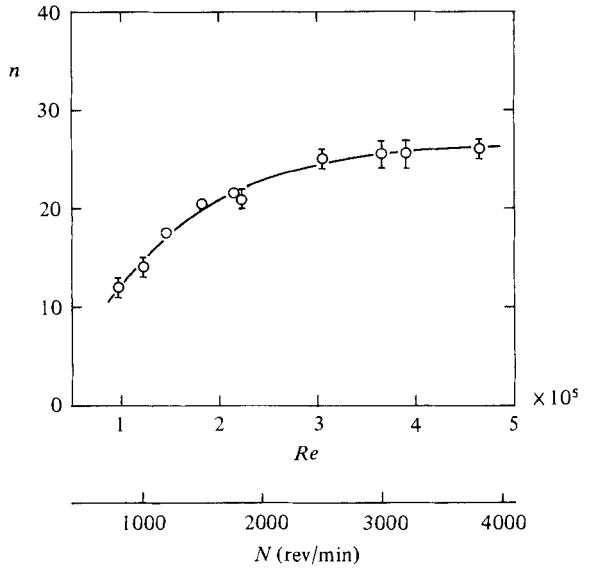

FIGURE 12. Number n of spiral vortices versus rotation speed N; $D = 250$ mm.

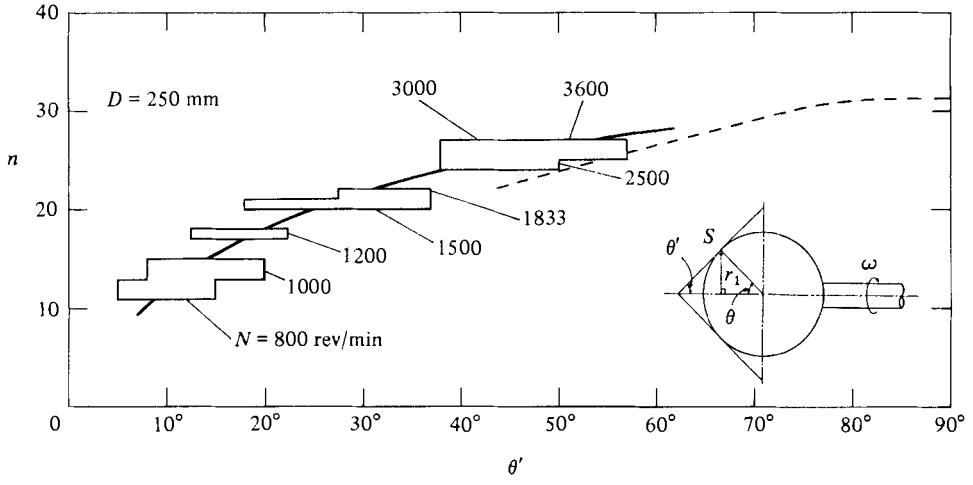

FIGURE 13. Comparison of the number n for a rotating sphere and for a rotating cone: ------, rotating cone.

Finally, figure 11 shows the local Reynolds numbers Re_{xc} and Re_{xt} for the transition regime versus the spin Reynolds number Re. It was found that the critical and the transition locations can be obtained from these similar curves, independent of the sphere size D and the rotation speed N.

3.3. *Spiral vortices*

Detailed measurements have been made of the spiral vortices, such as the number n of the vortices, the angle ϵ of the vortex axis and the breakdown process of the vortices to the turbulent state. Variation of the number n with the rotation speed N or the spin Reynolds number is shown in figure 12 for $D = 250$ mm. The number n was obtained by counting the spiral vortices in photographs taken from the

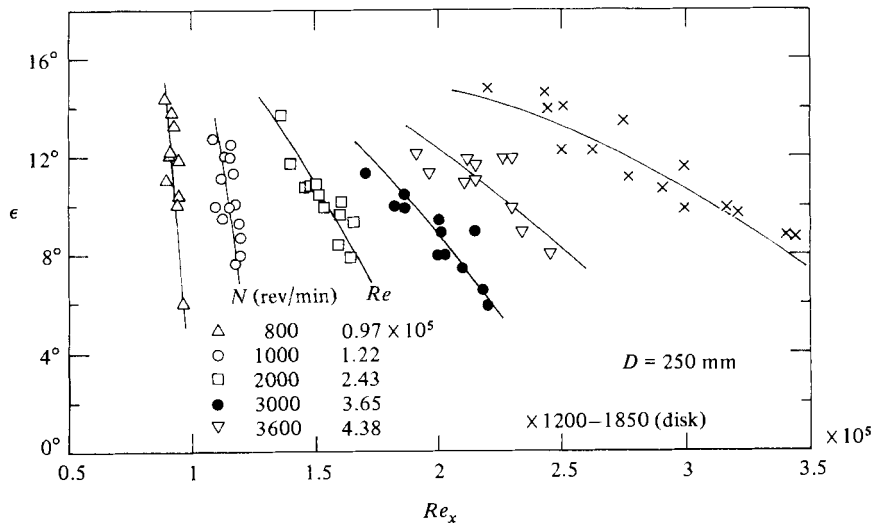

FIGURE 14. Comparison of the angle ϵ with that of a rotating disk: ×, rotating disk.

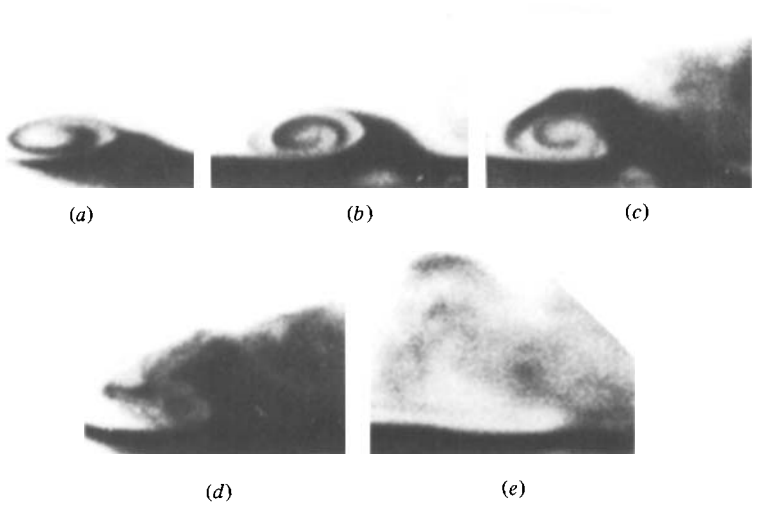

FIGURE 15. Breakdown process of the spiral vortex: $D = 250$ mm, $N = 1500$ rev./min.

direction of the axis of rotation. The value of n increases with the spin Reynolds number Re, and appears to approach asymptotically the value for the rotating disk ($n = 31$ or 32). The variation of n is a smooth process, and the n is uniquely determined against N.

It is known in the case of a rotating cone that n increases with its included angle (Kobayashi & Izumi 1979). It is interesting to compare the number n in these different-shaped rotating bodies. In figure 13 a comparison of the number n is shown for these two bodies. As explained in the figure, the number n of spiral vortices appearing at a point $S(\theta)$ on the sphere is compared with that of a rotating cone, which has a half-angle θ' ($= 90° - \theta$). The result shows reasonable agreement for $\theta' > 45°$.

The angle ϵ of the vortex axis was measured from visualized photographs and shown

in figure 14 versus the local Reynolds number. In the case $N = 2000$ rev./min, for example, it can be seen that at the beginning of boundary-layer instability the angle ϵ is about 14° and then gradually decreases to about 8° along the vortex axis. The tendency is almost the same for other values of N. That is, the angle ϵ decreases from about 14° at near-critical points to about 4°–8° at near-transition points. In the figure the data for the rotating disk (Kobayashi *et al.* 1980) are also plotted. It was noticed that the angle $\epsilon = 14°$ at the beginning of transition is almost independent of the rotation speed N (i.e. independent of position of the sphere). This differs greatly from the case of a rotating cone. In that case the angle ϵ decreases from 14° at the half-angle $\theta' = 90°$ to 0° at $\theta' = 15°$ (Kobayashi & Izumi 1979).

The breakdown process of spiral vortices is shown in figure 15. Photo (*a*) is a spiral vortex with single curl. Photo (*b*) is that with double curl. Photo (*c*) is a vortex accompanied by the superposed ring-like vortices shown in figure 4. Photo (*d*) is an almost-broken-down vortex from its top and inside. Photo (*e*) is a completely broken-down vortex.

4. Conclusions

Boundary-layer transition and the behaviour of the spiral vortices on different sizes of spheres rotating in otherwise undisturbed fluid were investigated experimentally. The results obtained are summarized as follows.

(i) Spiral vortices which appear in the transition regime of a sphere boundary layer are curling in the same direction. Ring-like vortices are superposed on the surface of spiral vortices just before the transition to turbulence. Spiral vortices begin to collapse from the surfaces and the inside of them after the appearance of several ring-like vortices.

(ii) The transition regime shifts from the equator toward the pole with increasing rotation speed N. The critical and the transition Reynolds numbers Re_{xc} and Re_{xt} for various sizes of spheres can be expressed with two curves shown in figure 11, if plotted against the spin Reynolds number Re based on sphere diameter.

(iii) The number n of spiral vortices increases with increasing rotation speed N, and appears to tend to the value for a rotating disk. The angle ϵ decreases from about 14° at near-critical points to about 4°–8° at near-transition points.

REFERENCES

BANKS, W. H. H. 1965 The boundary layer on a rotating sphere. *Q. J. Mech. Appl. Maths.* **18**, 443–454.

BANKS, W. H. H. 1976 The laminar boundary layer on a rotating sphere. *Acta Mech.* **24**, 273–287.

BOWDEN, F. P. & LORD, R. G. 1963 The aerodynamic resistance to a sphere rotating at high speed. *Proc. R. Soc. Lond.* A **271**, 143–151.

GREGORY, N., STUART, J. T. & WALKER, W. S. 1955 On the stability of three-dimensional boundary layers with application to the flow due to a rotating disk. *Phil. Trans. R. Soc. Lond.* A **248**, 155–199.

HOWARTH, L. 1951 Note on the boundary layer on a rotating sphere. *Phil. Mag.* **42**, 1308–1315.

ITO, A. 1980 The generation and breakdown of longitudinal vortices along a concave wall (in Japanese). *J. Japan Soc. Aeron. Space Sci.* **28**, 327–333.

KIRCHNER, R. P. & CHEN, C. F. 1970 Stability of time-dependent rotational Couette flow. Part 1. Experimental investigation. *J. Fluid Mech.* **40**, 39–47.

KOBASHI, Y. 1957 Measurements of boundary layer of a rotating sphere. *J. Sci., Hiroshima Univ.* A **20**, 149–157.

KOBAYASHI, R., KOHAMA, Y. & TAKAMADATE, C. 1980 Spiral vortices in boundary layer transition regime on a rotating disk. *Acta Mech.* **35**, 71–82.

KOBAYASHI, R., KOHAMA, Y. & KUROSAWA, M. 1983 Boundary-layer transition on a rotating cone in axial flow. *J. Fluid Mech.* **127**, 341–352.

KOBAYASHI, R. & IZUMI, H. 1983 Boundary-layer transition on a rotating cone in still fluid. *J. Fluid Mech.* **127**, 353–364.

KREITH, F. *et al.* 1963 Convection heat transfer and flow phenomena on rotating spheres. *Intl J. Heat Mass Transfer* **6**, 881–895.

MANOHAR, R. 1967 The boundary layer on a rotating sphere. *Z angew. Math. Phys.* **18**, 320–330.

NIGAM, S. D. 1954 Note on the boundary layer on a rotating sphere. *Z. angew. Math. Phys.* **5**, 151–155.

SAWATZKI, O. 1970 Das Strömungsfeld um eine rotierende Kugel. *Acta Mech.* **9**, 159–214.

SINGH, S. N. 1970 Laminar boundary layer on a rotating sphere. *Phys. Fluids* **13**, 2452–2454.

STEWARTSON, K. 1955 On rotating laminar boundary layers. *50 Jahre Grenzschichtforschung, Freiburg i. Br.*, pp. 59–71.

THEODORSEN, T. & REGIER, A. 1944 Experiments on drag of revolving disks, cylinders, and streamline rods at high speeds. *NACA Rep.* 793, pp. 367–384.

WALOWIT, J., TSAO, S. & DIPRIMA, R. C. 1964 Stability of flow between arbitrarily spaced concentric cylindrical surfaces including the effect of a radial temperature gradient. *Trans. ASME* E: *J. Appl. Mech.* **31**, 585–593.

YAMABE, H., NISHIDA, S. & ITO, J. 1982 Laminar boundary layer on a rotating sphere (in Japanese). *Bull. Japan Soc. Mech. Engrs* **239**, 62–64.